Hindawi
International Journal of Corrosion
Volume 2022, Article ID 7218063, 15 pages
https://doi.org/10.1155/2022/7218063

Research Article

Anticorrosive Effect of Halogenated Aniline Enaminoesters on Carbon Steel in HCl

Mariana F. P. Carlos, Geicy K. P. Barboza, and Aurea Echevarria

Department of Organic Chemistry, Institute of Chemistry, Federal Rural University of Rio de Janeiro, Seropedica 23.890-000, Brazil

Correspondence should be addressed to Aurea Echevarria; echevarr@ufrrj.br

Received 22 February 2022; Revised 15 April 2022; Accepted 20 April 2022; Published 27 May 2022

Academic Editor: Michael J. Schütze

Four enaminoesters derived from halogenated aniline, with potential anticorrosion activity, were synthesized and tested against carbon steel AISI 1020 in acid medium using 1.0 mol L^{-1} HCl. The synthesis was demonstrated through the reaction of ethyl acetoacetate with four different amines, in the presence of glacial acetic acid and molecular sieve, using ethanol as solvent for 24 h. The evaluation of the anticorrosive activity was performed using the gravimetric technique and electrochemical methods, such as electrochemical impedance spectroscopy (EIS), linear polarization resistance (LPR), and potentiodynamic polarization (PP). Results indicated that the F-EN (Ethyl (2*Z*)-3-[(4-fluoro-phenyl)-amino]-but-2-enoate) inhibitor had higher corrosion inhibition efficiency, of 98% by mass loss, and 85% by electrochemical techniques. Adsorption obeyed the Langmuir isotherm, thus suggesting that the inhibitors form a monolayer film in metal surface. These results also contributed to the calculations of the physicochemical parameters of E_a, $\triangle H^{\neq}_{ads}$, and $\triangle S^{\neq}_{ads}$, which confirmed the corrosion inhibition when compared to the absence of the inhibitors.

1. Introduction

Corrosion is the process of spontaneous deterioration of a material that affects several industrial segments globally, causing major economic problems such as replacement of equipment, and thus needs investigation for its control [1–3]. Due to the mechanical properties of carbon steel, of its low cost, and being easily handled, it is generally used in different industries, such as production, chemical processing, petroleum transportation, and refining, thus being exposed to salts, gases, and acids, and consequently, conditioned to many corrosive processes [4, 5]. Its susceptibility to corrosion reinforces the importance of developing new efficient methods of combating it; however, their efficiency is conditioned to the comprehension and characterization of the various corrosive media accountable for the deterioration of the material [6, 7].

Although there are several methods to protect against the corrosive environment, the use of corrosion inhibitors has been widely used due to low cost, simple process, strong adaptability, and economic efficiency [1]. Inhibitors are organic or inorganic substances that can reduce or eliminate corrosion, slowing down the anodic and/or cathodic reactions on the metal surface [6, 8]. The use of organic molecules as inhibitors is already widely studied as a promising alternative since they associate with the metal by adsorption, thus protecting the surface [9, 10]. Physical adsorption involves electrostatic interaction between inhibitory agents and the metal surface, whereas chemical adsorption involves charge splitting or electron transfer from the organic molecule to the metal surface [11]. The adsorption properties are related to the presence of unsaturation (π electrons) and the presence of heteroatoms, such as nitrogen and oxygen, where the transfer of their nonbonding electron pairs to the d orbitals of the Fe atoms on the metal surface, by a coordinated bond, causing the surface of the metal to be covered [12–15].

Enaminoesters are common representatives of the enaminones class, which refers to compounds that have the conjugated bonds (N-C=C-C=O), combining the nucleophilicity of enamines with the electrophilicity of enones, thus being considered very versatile intermediates [16]. These compounds have structures with electronic acceptor-donor

electronic effects, and their reactivity action is due to the resonance effect of the acyl and amine moieties on the double bond, where the π electrons displacement resulting from this effect leads to a noticeable polarization of the olefinic carbons [6].

Enaminoesters are considered potential corrosion inhibitors because of their structural similarity to the Schiff bases, which had previously shown positive results against corrosion in studies such as Heydari's (2018) that investigated two Schiff bases as inhibitors of corrosion against carbon steel in HCl with 97% and 88% of efficiencies [11].

Recently, gravimetric and electrochemical methods were first used by Carlos (2018), who studied the application of two β-enaminoesters as corrosion inhibitors in acid medium using 0.5 mol L^{-1} HCl against carbon steel. Both compounds ethyl (2*Z*)-3-[(2-phenylethyl)-amino]-but-2-enoate and ethyl (2*Z*)-3-{[2-(4-methoxyphenyl)-ethyl]-amino}-but-2-enoate showed good inhibition efficiency, but the first presented a better result, with 98% inhibition in a 24 h of immersion in concentration of 1.0×10^{-2} mol L^{-1} by weight loss method [6]. Furthermore, only this article has been published, so far, involving the anticorrosion activity of enaminoesters. These compounds have been investigated as intermediates in the synthesis of other compounds, including the class of heterocyclics, also aiming at their biological potential [17–20].

Thus, the results obtained for enaminoesters as new anticorrosive agents highlight them for a scientific advance in the search for new inhibitors. Considering this information, in this work, four β-enaminoesters derived from halogenated anilines were synthesized to evaluate their anticorrosion action against AISI 1020 carbon steel in 1.0 mol L^{-1} HCl to compare with the nonsubstituted anilino-β-enaminoester. The compounds ethyl (2*Z*)-3-[(4-X-phenyl)amino]-but-2-enoate, where X = H (H-EN), Cl (Cl-EN), Br (Br-EN), and F (F-EN), were evaluated regarding their anticorrosive effects using the gravimetric method of mass loss, and electrochemical methods, such as linear polarization resistance (LPR), electrochemical impedance spectroscopy (EIS), and potentiodynamic polarization (PP).

2. Materials and Methods

2.1. Reagents and Materials. The reagents used in this work for the synthesis of β-enaminoesters were ethanol from Neon and aniline 99%, 4-chloroaniline 98%, 4-fluoroaniline 99%, 4-bromoaniline 97%, and ethyl acetoacetate 99%, from Sigma-Aldrich. All reagents were used lacking prior treatment. For electrochemical measurements and gravimetric testes, ethanol and hydrochloric acid were purchased from Neon and Sigma-Aldrich, respectively.

2.2. Synthesis. Halogenated aniline β-enaminoesters were synthesized by mixing ethyl acetoacetate, the corresponding substituted aniline, drops of glacial acetic acid, 4 MSDS (Molecular sieves), and ethanol in a round bottom flask. The mixture remained in magnetic stirring for approximately 24 h at 30°C. Figure 1 shows the synthesis route used to obtain the halogenated 4-X-anilino-β-enaminoesters.

2.3. Characterization. Ethyl (2*Z*)-3-anilino-but-2-enoate (H-EN)

Light yellow oil; η_p=1.582; FT-IR (ν cm^{-1}) 3261, 2832, 1694, 1650, 1494, 1267, 1161/1060; ^{1}H NMR ($CDCl_3$, ppm) δ 11.7, 7.17, 6.98, 6.90, 4.58, 4.08, 2.20, 1.22; ^{13}C NMR DEPTQ 135 ($CDCl_3$, ppm) δ 172.1, 161.5, 138.1, 128.5, 125.5, 125.2, 91.2, 59.1, 20.6, 14.3.

Ethyl (2*Z*)-3-[(4-chloro-phenyl)-amino]-but-2-enoate (Cl-EN) [21]

Brown oil; η_p=1.4875; FT-IR (ν cm^{-1}) 3369, 2979, 1616, 1593, 1492, 1265, 1091, 1161/1058, 821; ^{1}H NMR ($CDCl_3$, ppm) δ 10.36, 7.27, 6.58, 4.72, 4.15, 1.96, 1.28; ^{13}C NMR DEPTQ 135 ($CDCl_3$, ppm) δ 170.4, 158.5, 136.9, 130.2, 129.0, 125.4, 86.9, 58.9, 20.2, 14.5.

Ethyl (2*Z*)-3-[(4-bromo-phenyl)-amino]-but-2-enoate (Br-EN) [22]

White solid; M.P.=53°C (lit. 54°C); FT-IR (νcm^{-1}) 3280, 2979, 1712, 1614, 1591, 1488, 1265, 1020, 1070, 819; NMR ^{1}H ($CDCl_3$ ppm) δ 10.36, 7.42, 6.55, 4.73, 4.16, 1.98, 1.28; NMR ^{13}C DEPTQ 135 ($CDCl_3$, ppm) δ 170.4, 158.3, 138.5, 137.7, 131.9, 125.7, 116.7, 87.2, 58.9, 20.2, 14.6.

Ethyl (2*Z*)-3-[(4-fluoro-phenyl)-amino]-but-2-enoate (F-EN) [23]

Light brown oil; η_p=1.4720; FT-IR (ν cm^{-1}) 3282, 1650, 1610, 1510, 1359, 1269, 1230/1153; ^{1}H NMR ($CDCl_3$, ppm) δ 10.24, 7.03, 6.86, 4.71, 4.10, 1.93, 1.20; ^{13}C NMR ($CDCl_3$, ppm) δ 170.5, 161.6, 159.3, 135.2, 126.8, 115.7, 85.8, 58.8, 20.1, 14.6.

2.4. Evaluation of Anticorrosion Activity

2.4.1. Test Solutions. Acid medium was prepared diluting analytical commercial HCl 37% with Milli-Q water to 1 mol L^{-1}. The corrosion experiments were performed without the synthesized inhibitors (blank solution) and in the presence of different concentrations of the enaminoesters ranging from 10^{-2} to 10^{-5} mol L^{-1}. The electrochemical assays were carried out under air atmosphere without stirring and the temperature of the solutions was around 30°C and for the weight loss tests, the temperature was controlled at 30, 40, 50, and 60°C.

2.4.2. Electrochemical Measurements. A corrosion cell kit with three electrodes was used: the reference electrode was an Ag/AgCl (3 M KCl), the auxiliary electrode was a platinum electrode, and the working electrode was a mild steel AISI 1020 of 1 cm^2. The working electrode was abraded with 400, 600, and 1200-grade emery paper, washed with distilled water, degreased with ethanol, and dried by hot air. Electrochemical impedance spectroscopy (EIS), linear polarization resistance (LPR), and potentiodynamic polarization (PP) measurements were analyzed with NOVA 2.1 software and carried out using the Autolab Potentiostat/Galvanostat model PGSTAT 302N. The open circuit potential (OCP) was managed in the test solution for 1 h until stabilization was observed. EIS spectra were obtained using a frequency range of 10 KHz -0.1 Hz with an amplitude of 10 mV peak-by-peak in different concentrations, having 50 frequency points logarithmically spaced throughout the

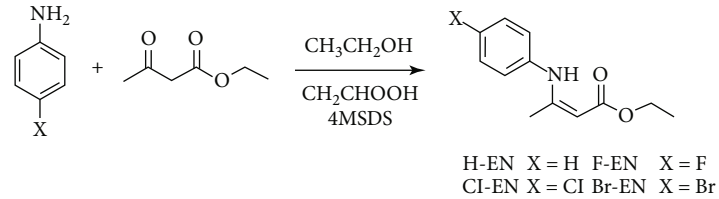

Figure 1: Synthesis of halogenated anilino-β-enaminoesters.

frequency range to be measured. The impedance data were interpreted in equivalent electrochemical circuit, being adjusted in the NOVA program, and it were calculated using Equation (1) [24].

$$\eta_{EIS} = \frac{R_{ct\,(inh)} - R_{ct}}{R_{ct\,(inh)}} \times 100, \quad (1)$$

where $R_{ct(inh)}$ is the charge transfer resistance in the solution with the inhibitors; R_{ct} is the charge transfer resistance in the blank solution.

LPR assays were carried out by a scan rate of 1 mV s^{-1} in the potential range of ±10 mV from the open circuit potential (OCP) starting from more cathodic potential to anodic ones and its efficiency was calculated using Equation (2) [25].

$$\eta_{RPL} = \frac{R_{p\,(inh)} - R_p}{R_{p\,(inh)}} \times 100, \quad (2)$$

where $R_{p(inh)}$ is resistance of polarization in the presence of the inhibitor, and R_p is the resistance in the absence of the inhibitor.

PP curves were carried out in the potential range of ±200 mV versus OCP using a scan rate of 1 mV s^{-1} and the polarization resistance (R_p) was obtained from the incline of the obtained potential; the efficiency of this test was calculated using Equation (3) [4].

$$\eta_{PP} = \frac{i^0_{corr} - i_{corr}}{i^0_{corr}} \times 100, \quad (3)$$

where i^0_{corr} is the uninhibited corrosion density and i_{corr} is the inhibited corrosion current density.

The assays were performed three times to assure the repeatability under each experimental condition. The surface analysis was also performed with scanning electronic microscopy applying a Hitachi TM 3000 tabletop microscope after a 24 h immersion time at room temperature.

2.4.3. Gravimetric Measurements. The weight loss tests were taken using specimens of 3.0 × 3.0 × 0.15 cm, abraded with a different sandpapers grade, and cleaned with distilled water and ethanol. The steel specimens were subjected to different immersion times (3 h, 6 h, 24 h, and 48 h) in the lack and presence of the inhibitor. Temperature effect was evaluated by repeating the assays at 30, 40, 50, and 60°C, using 1 × 10^{-2} mol L^{-1} which was the concentration where the inhibitors showed greater efficiency. The inhibition efficiency was calculated using Equation (4) [24].

$$\eta_{WL} = \frac{\text{Corrosion rate} - \text{Corrosion rate}_{inh}}{\text{Corrosion rate}} \times 100, \quad (4)$$

where corrosion rate and corrosion rate_{inh} in the absence and presence of the studied inhibitors, respectively.

All tests, weight loss and electrochemical assays, were made at least in triplicate under same conditions and the accepted values with difference smaller of 2%, indicating good reproducibility. The mean of results was used.

2.4.4. Theoretical Calculations. The theoretical descriptors were used to establish correlations with the corrosion inhibition efficiency refer to the Theory of Molecular Boundary Orbitals (FMO), where the energy of the HOMO orbital can be associated with the ability of the molecule to donate electrons to the metallic surface, while the energy of the LUMO orbital refers to the molecule's susceptibility to receive electrons. The descriptor dipole moment (μ) was used to describe the polarity of molecules and correlate with its inhibition efficiency [26]. The SPARTAN 14 program was used to perform the theoretical calculations and the PM6 semi-empirical method to correlate the highest inhibition efficiency.

3. Results and Discussion

3.1. Synthesis. The synthesis of β-enaminoesters was based on the previously reported procedures [6, 27]. In this work, the preparation was performed with small modifications via acid catalysis, using glacial acetic acid to favor the activation of the ethyl acetoacetate carbonyl, making the substituted aniline attack easier, and thus resulting in the product of interest. The compounds H-EN, Cl-EN, and F-EN were obtained in the form of oil and the Br-EN as amorphous solid. All compounds were soluble in the ethanol-water mixture and characterized by spectroscopic data, according to the literature [21–23]. Table 1 shows the yield values, refractive indices, or melting point of the synthesized enaminoesters.

3.2. Electrochemical Impedance Spectroscopy (EIS). The EIS assays were performed using the 1.5 cm × 1.5 cm AISI carbon steel working electrode in 1.0 mol L^{-1} HCl. The concentrations of the enaminoesters to be tested were 1.0 × 10^{-2}, 1.0 × 10^{-3}, 1.0 × 10^{-4}, and 1.0 × 10^{-5} mol L^{-1} and diluted in ethanol/Milli-Q water solution (7 : 3). The tests were carried through at a stable open circuit potential (OCP) at 30°C and after 1 h of exposure in the corrosive medium.

Table 1: Yields, melting points (M.P.), and refractive indices (η_p) for the synthesized β-enaminoesters.

Compound	Yield (%)	η_p	M.P. (°C)
F-EN	81	1.4720	—
Cl-EN	72	1.4875	—
Br-EN	68	—	53
H-EN	92	1.582	—

The diagrams obtained using the EIS technique for halogenated enaminoesters were drawn using E_{corr} values at different concentrations, as mentioned above, in the presence and absence of the inhibitors and evaluated by Nyquist plots (Figure 2).

The Nyquist diagrams (Figure 2) showed a single semicircle that changed along the axis of the real impedance (Z') indicating that the corrosion of carbon steel was commanded by a charge transfer process with extremely low diffusional effect and was not considered. The charge transfer resistance (R_{ct}) values were obtained from Z'. The inhibition efficiency gets higher with increasing concentration of inhibitor, which is shown by the bigger semicircle of Figure 2 and corroborated by the results in Table 2 which presents the values of electrochemical parameters such as the resistance of polarization (R_P), electrical double-layer capacitance (C_{dl}), and efficiency of inhibition (EI%) for different concentrations of enaminoesters. Moreover, it is also observed that the diameters of the Nyquist diagrams in the presence of enaminoesters are larger compared to the diameter of the diagram of Nyquist in the absence of the inhibitor. This observation suggests that the presence of inhibitor agents in a corrosive environment imposes an inhibiting barrier for charge transfer reactions that occur at the metal-electrolyte interface. In other words, the deposit of protective layer slows down the process of charge transfer [4, 12, 16, 28].

Furthermore, it is observed that in the Nyquist diagram (Figure 2), there is no change in the shape of the curve in the absence of inhibitor in relation to the shape of the curves in the presence of enaminoesters, indicating that the inhibitors adsorb on the metal surface, but they do not alter the metal's corrosion mechanism.

The equivalent $R(RC)$ electric circuit for the impedance curves was represented from the simpler equivalent circuit (Figure 3), Randles circuit, which is a parallel mixing of charge transfer resistance (R_{ct}) and double-layer capacitance (C_{dl}), both in series with the solution resistance (R_s).

Bode's diagrams for the anticorrosive effects of the synthesized enaminoesters corroborate the results obtained with the Nyquist plots, as there is an increase in total impedance (Z) with the frequency. The increase in the total impedance (Z) is consistent with the results obtained with the Nyquist diagrams, since at low frequencies the resistance increased with time. The frequency versus phase angle graphs shows that the increase in the contact time of carbon steel with the solution containing the enaminoesters led to the maximum phase angle, which also indicated an increase in capacitance [29, 30].

The double-layer capacitance was calculated from the impedance, represented by Z, which measures the relation between E and i using the imaginary part, obtained at high frequencies (10 kHz), due to the minimum presence of flaky processes in them. The C_{dl} was calculated using Equation (5) [31–33].

$$C_{dl} = \frac{1}{2\pi f Z_{im} A}, \tag{5}$$

where f is the frequency of 10000 Hz, Z_{im} is the imaginary component at the frequency of 10000 Hz, and A is the electrode area in cm^2, which, in the case of this work, was 1 cm^2. Table 2 shows the electrochemical parameters obtained for the synthesized enaminoesters by means of EIS tests.

The electrical double-layer capacitance (C_{dl}) was another parameter used. The determination was made considering the frequency at which the imaginary component is maximum and observing the double-layer capacitance increase due to the presence of the inhibitor on the surface, thus increasing the load density at the metal and solution interface. The increase in R_{ct} and the decrease in C_{dl} indicated that these compounds inhibited corrosion on carbon steel by an adsorption mechanism [5, 6, 33].

It is observable in Table 2 that the maximum efficiency, 85%, was seen in the compound F-EN at 1.0×10^{-2} mol L^{-1} where the lowest C_{dl} value was found. When there is a formation of a protective film at the metal/solution interface, it can be observed an increase in R_{ct} value. The decrease in C_{dl} with the increase in inhibition efficiency may be provoked by the decrease in the dielectric constant and/or increase the thickness of the electrical double-layer, indicating that the mechanism is adsorptive to the metal surface [4, 34]. Also, this decrease can indicate the gradual replacement of water molecules by inhibitor molecules on the steel surface, which modifies the structure of the double electrical layer [35].

Bode's diagrams for the synthesized enaminoesters provide information related to the behavior of the protective film formed on the electrode because of inhibitor adsorption and it confirms the increase in the total impedance (Z) with the frequency, corroborate with the results obtained in the Nyquist diagrams, since at low frequencies the resistance increased with time (Figure 4). The frequency versus phase angle graphs shows that the increase in carbon steel contact time with the solution containing the enaminoesters led to the maximum phase angle, which also indicated an increase in capacitance [27, 36, 37].

3.3. Linear Polarization Resistance (LPR). The measures were evaluated in the presence of the synthesized inhibitors and in the absence of them (blank solution). The values obtained for the current density (i) versus applied potential (E), which provided the incline of the lines corresponding to R_p values by linear regression application, are in Table 3, together with the values of anticorrosion efficiency values.

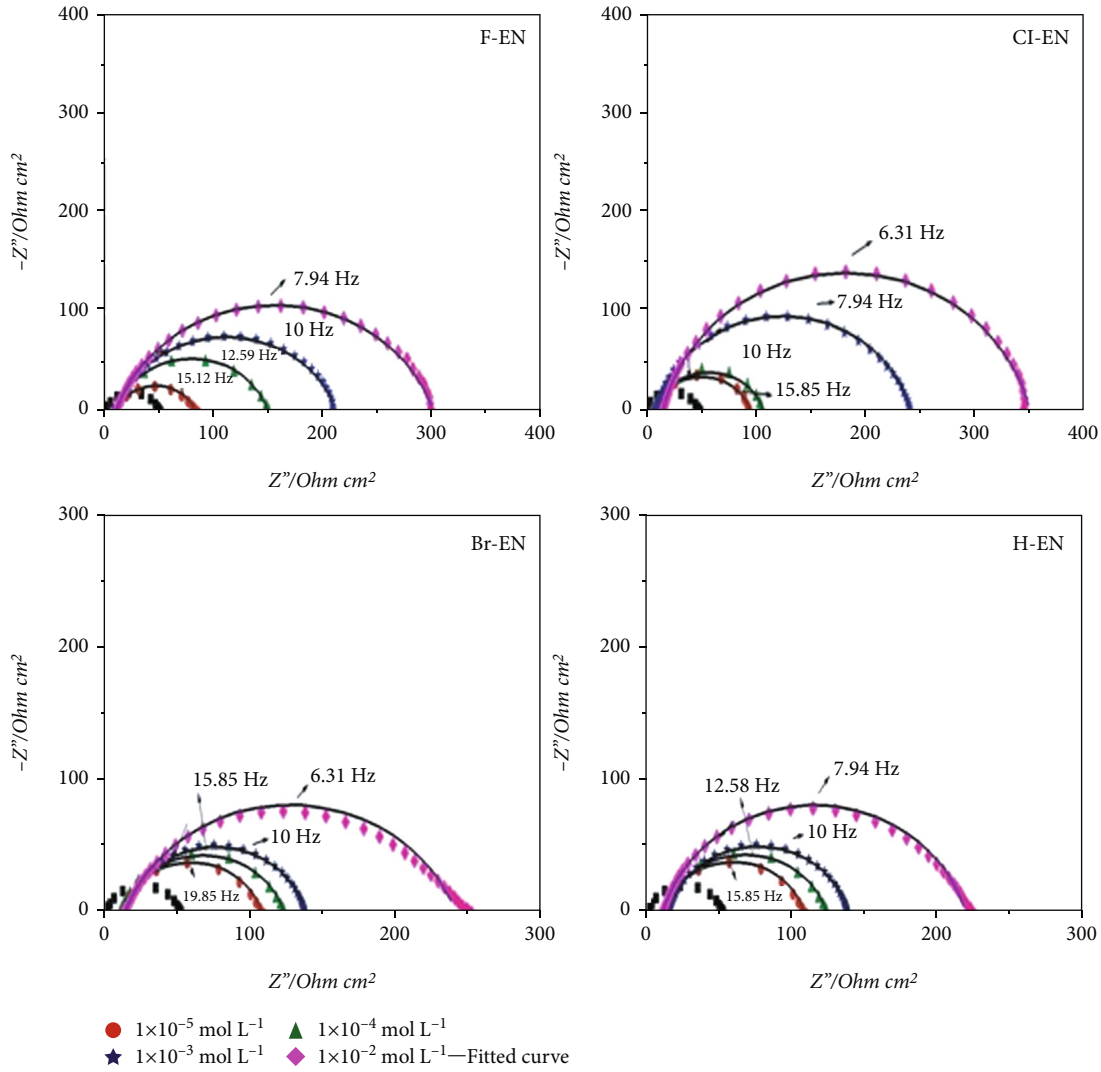

Figure 2: Nyquist plots obtained in absence and presence of inhibitors against AISI 1020 carbon steel in 1.0 mol L^{-1} HCl.

The inhibition efficiency is characterized by the difference between the R_p of the experiment in the blank solution and in the solution with the presence of the inhibitors. In these experiments, the rise in concentration led to an increase in the anticorrosion efficiency, thus indicating the highest inhibition in 1.0×10^{-2} mol L^{-1} for all compounds, as shown in Table 3, which corroborates with the results obtained by the EIS technique.

Although the anticorrosion efficiency is not extremely high, 85.0% for the most efficient compound (F-EN) at 10^{-2} mol L^{-1}, this result is satisfactory because its synthesis, as well as to the other evaluate compounds, is simple and fast and uses water as solvent making an ecofriendly route. Furthermore, all electrochemical test and the weight loss showed correlated results.

3.4. Potentiodynamic Polarization Measurement (PP). PP curves of carbon steel AIS 1020 in 1.0 mol L^{-1} HCl solutions, in blank corrosive solution, and in the presence of β-enaminoesters are shown in Figure 5, at four concentrations. PP technique was used, specially, to observe the inhibitor type such as anodic, cathodic, or mixed.

The polarization curves for Cl-EN and Br-EN underwent a slight displacement of E_{corr} in the cathodic side, suggesting that the addition of compounds in the solution decreased the oxidation of the steel and delayed the cathodic evolution of hydrogen. Thus, the inhibitors Cl-EN and Br-EN can be classified as mixed corrosion inhibitors with a cathodic tendency in an acid medium, and H-EN with a small displacement [31, 32]. The F-EN compound, on the other hand, presented a slight displacement towards the anodic region at higher concentration, thus being classified as a mixed inhibitor agent with anodic tendency.

The PP electrochemical tests were performed for the synthesized enaminoesters, at different concentrations, under the same working conditions as EIS and LPR tests. The Tafel curves for the carbon steel electrode in HCl 1.0 mol L^{-1} obtained are shown in Figure 5. The parameters

Table 2: Electrochemical parameters obtained through EIS tests of AISI 1020 carbon steel in 1.0 mol L^{-1} HCl medium at different concentration of enaminoesters.

Inhibitor	Conc. (Mol L^{-1})	OCP/ag/AgCl (mV)	R_{ct} (Ω cm^2)	R_s (Ω cm^2)	Θ	n	C_{dl} (μF cm^2)	η_{EIs} (%)
Blank	—	—	51.63	6.47	—		537	—
F-EN	1.0×10^{-5}	-0.470	73.02	10.36	0.4015	0.99	28.54	40.2
	1.0×10^{-4}	-0.437	140.10	9.91	0.6583	0.96	25.20	65.8
	1.0×10^{-3}	-0.432	204.61	10.18	0.7936	0.99	19.96	79.4
	1.0×10^{-2}	-0.403	295.82	9.74	0.8478	0.97	15.81	85.4
Cl-EN	1.0×10^{-5}	-0.500	86.91	9.69	0.4583	0.88	29.48	46.2
	1.0×10^{-4}	-0.502	98.41	9.71	0.5204	0.98	27.16	52.2
	1.0×10^{-3}	-0.473	231.26	10.86	0.7476	0.89	25.76	74.8
	1.0×10^{-2}	-0.462	336.85	10.21	0.8311	0.90	20.29	83.1
Br-EN	1.0×10^{-5}	-0.485	93.45	11.35	0.5188	0.96	9.85	52.3
	1.0×10^{-4}	-0.486	109.02	11.29	0.5786	0.97	9.37	57.9
	1.0×10^{-3}	-0.477	127.76	10.88	0.6373	0.97	9.17	62.9
	1.0×10^{-2}	-0.459	228.38	11.59	0.7918	0.95	9.06	79.8
H-EN	1.0×10^{-5}	-0.452	61.43	9.92	0.4115	0.89	125.35	41.1
	1.0×10^{-4}	-0.479	93.33	10.83	0.5189	0.92	100.26	51.9
	1.0×10^{-3}	-0.466	176.86	9.05	0.7080	0.91	29.73	69.8
	1.0×10^{-2}	-0.457	233.86	11.04	0.7909	0.88	19.27	79.4

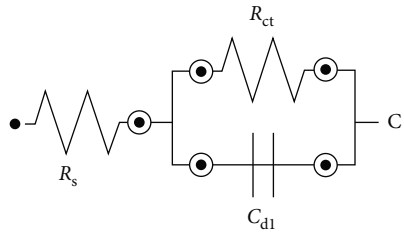

Figure 3: Equivalent circuit for the inhibitors.

associated to polarization curves, such as corrosion potential (E_{corr}), corrosion current density (j_{corr}), and anodic and cathodic Tafel constants (β_a and β_c, respectively), were obtained via extrapolation of the linear portions of curves from anodic and cathodic polarization lines [38]. Also, the inhibition efficiency IE (%) is shown in Table 4. The results of the potentiodynamic polarization inhibition efficiency and its parameters can be seen in Table 4.

The polarization curves show that the corrosion current density values decreased with the addition of compounds when compared to blank solution suggesting that the enaminoesters own protective capacity to carbon steel in acidic medium [39]. The decrease in the corrosion current density with increased concentration of enaminoesters can be explained by the increased adsorption of these compounds on the metal surface indicating the formation of a protective layer formed [31, 40].

The inhibition efficiency values calculated by PP method showed good correlation with the EIS and LPR results, in which the compound F-EN was also the more efficient among all.

3.5. Gravimetric Measurements. The weight loss tests were carried through at the concentration of 1.0×10^{-2} mol L^{-1}, because this was the concentration that the inhibitors showed the highest efficiency, in HCl 1.0 mol L^{-1} solution against carbon steel AISI 1020. The tests were carried out, first, with time variation of immersion (3 h, 6 h, 24 h, and 48 h) at the same temperature of 30°C and, later, with temperature variation of 30°C, 40°C, 50°C, and 60°C, using a thermostatic bath. The corrosion inhibition efficiency was calculated from Equation (4), and in Table 5 are the results obtained from the mass loss tests, according to the immersion time change.

A decrease of W_{corr} with the increase in immersion time for the four inhibitors was observed, as shown in Figure 6.

The corrosion rates obtained in the tests with the presence of the inhibitors were lower than in their absence (Table 6), thus confirming the inhibitory effect of the synthesized enaminoesters through the formation of a coating layer on the metal surface [33]. These values are correlated to the inhibition efficiency, observed by the great difference between the corrosion rate of inhibitors when compared to blank. The anticorrosive potential of the synthesized inhibitors can be justified due to the availability of heteroatoms like nitrogen with their nonligand electrons, and the aromatic rings with their π-electrons [41, 42]. The compounds F-EN, Cl-EN, and Br-EN showed 98% inhibition efficiency after 48 h of immersion, and H-EN, 92% in same immersion time, thus indicating the importance of the presence of the halogen moiety.

Values of W_{corr} decreased with the increase in immersion time for the F-EN and Cl-EN inhibitors, as shown in Figure 6, despite achieving its stability in 24 h. On the other hand, the compounds Br-EN and H-EN showed decrease of corrosion rate in 48 h of immersion. The high inhibitive performance of F-EN and Cl-EN suggests a higher bonding ability of these halogenated compounds on mild steel surface. However, the larger size of the bromine moiety in Br-EN and the unsubstituted phenyl ring of H-EN led to higher corrosion rates and consequently lesser inhibitory effects.

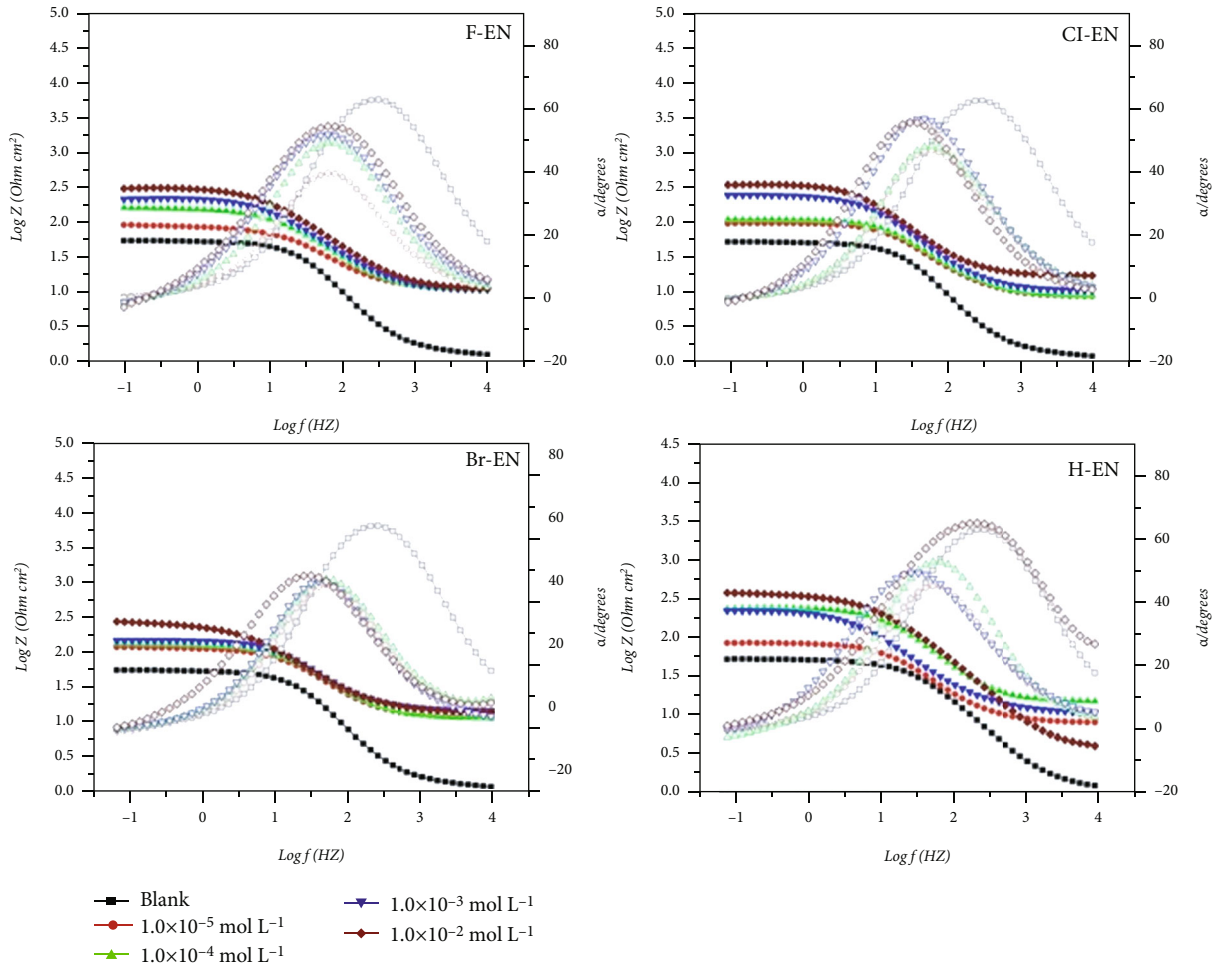

FIGURE 4: Bode's impedance plots for the carbon steel obtained in 1 mol L^{-1} HCl in the presence and absence of the inhibitors.

The temperature effect was also evaluated in the mass loss tests. The tests were performed in compound concentration of 1.0×10^{-2} mol L^{-1} against AISI 1020 carbon steel at 30°C, 40°C, 50°C, and 60°C in the presence of 1.0 mol L^{-1} HCl, after 3 h of immersion time. The results acquired for corrosion inhibition efficiency according to temperature variation are shown in Table 6. These data were obtained using the Arrhenius equation, ln W_{corr} versus 1/T, as shown in Figure 7, which permitted the calculation of the E_a (activation energy) of the corrosion process. Thus, E_a was calculated as shown in Equation (6).

$$\ln W_{corr} = -\frac{E_a}{R.T} + \ln A, \tag{6}$$

where W_{corr} is the corrosion rate, E_a the activation energy, A the frequency factor, T the temperature (K), and R is the gas molar constant.

Comparing the inhibition efficiencies obtained by the different electrochemical methods, we can see that they were reasonably similar, with the F-EN compound always being the most efficient, being PP (84.8%), LPR (85.0%), and EIS (85.4%). Furthermore, when comparing the electrochemical methods with the mass loss method in 3 hours of immersion, we also observed similar results, with F-EN being the most efficient with 85.6% efficiency.

The working temperature can influence the efficiency of the corrosion inhibition [34]; Table 7 shows that when temperature rises, there is an increase in W_{corr} and a decrease of inhibition efficiency. However, this increase is greater in the absence of inhibitors and, from the values of the inhibition efficiency with increasing temperature, it appears that they decrease, being characteristic of a physisorption process. The increase in temperature can cause an increase in the kinetic energy and mobility of the inhibitor molecules, tending to intensify the corrosive process. The compound that showed the best corrosion inhibition at 60°C was Cl-EN (64%).

Complementarily to the Arrhenius equation, two other physical-chemical parameters can be determined, adsorption activation enthalpy ($\Delta H^{\neq}_{ads}$) and adsorption activation entropy ($\Delta S^{\neq}_{ads}$), from the Eyring equation, which is shown in Equation (7). Table 7 shows the thermodynamic parameter values obtained by Arrhenius and Eyring equations.

$$\ln \frac{W_{corr}}{T} = \ln \left[\frac{K_b}{h} e^{\triangle S \neq / R}\right] - \frac{\triangle H \neq}{R.T}, \tag{7}$$

Table 3: Electrochemical parameters obtained from LPR tests for halogenated aniline β-enaminoesters in 1.0 mol L^{-1} HCl medium in AISI 1020 carbon steel.

Inhibitor	Conc. (mol L^{-1})	r^{2a}	R_p (Ω cm^2)	Θ	η_{RPL} (%)
Blank	—	0.999	51.79	—	—
F-EN	1.0×10^{-5}	0.999	90.79	0.4295	43.2
	1.0×10^{-4}	0.998	165.02	0.6810	68.6
	1.0×10^{-3}	0.997	202.02	0.7436	74.4
	1.0×10^{-2}	0.997	273.32	0.8505	85.0
Cl-EN	1.0×10^{-5}	0.999	93.03	0.4433	44.3
	1.0×10^{-4}	0.999	106.34	0.5130	51.4
	1.0×10^{-3}	0.998	235.92	0.7805	78.0
	1.0×10^{-2}	0.998	339.89	0.8076	81.8
Br-EN	1.0×10^{-5}	0.999	117.16	0.5579	55.8
	1.0×10^{-4}	0.999	126.12	0.5893	58.9
	1.0×10^{-3}	0.999	142.75	0.6372	63.7
	1.0×10^{-2}	0.998	236.11	0.7806	78.1
H-EN	1.0×10^{-5}	0.8594	445.55	0.4944	49.1
	1.0×10^{-4}	0.8318	772.96	0.5085	51.3
	1.0×10^{-3}	0.8642	1268.8	0.7224	72.1
	1.0×10^{-2}	0.8383	2467.6	0.8087	80.8

where W_{corr} is the corrosion rate, K_b Boltzmann constant, h the Planck constant, $\Delta H^{\neq}$ the enthalpy, $\Delta S^{\neq}$ the entropy, and R is the gas molar constant.

In accordance with the Arrhenius graph, ln W_{corr} versus 1/T (Figure 7), and the results generated in Table 7, after linear regression application, favorable values of correlation coefficient were observed in the range of 0.99997 and 0.99935, for the experiments in the presence of inhibitors.

Adsorption activation enthalpy and adsorption activation entropy were determined from the Eyring equation (Equation (7)). In addition, by observing Table 7, it is possible to see an increase in E_a and $\Delta H^{\neq}$ values in the presence of inhibitors, which means the required energy barrier to initiate a corrosive process is higher, thus justifying the inhibitory action of the synthesized compounds. The increase of E_a and $\Delta H^{\neq}$ values when compared to blank indicates the prevention of the charge or mass transfer reaction occurring on the surface [35]. The increase of E_a also suggests that the rate of carbon steel dissolution decrease due to formation of a metal: inhibitor complexes as according to the literature [43, 44].

After increasing the temperature, the lowest in the efficiency was observed, which might be related to by the decreased electrostatic forces between the enaminoester and the surface [45, 46], and that the physical adsorption occurs at first stage of adsorption process [47, 48]. Higher $\Delta S^{\neq}$ values were observed in the presence of inhibitor agents when compared to without, as well as a lower number of negative values, suggesting as a result a higher disorder due to displacement of water molecules and chloride ions through the interaction of the enaminoester with the surface. The negative values suggest a decrease of perturbation associated to the interaction of inhibitors on metal surface [49, 50].

3.6. Adsorption Isotherm. One of the most convenient ways of expressing adsorption quantitatively is by deriving the adsorption isotherm that characterizes the metal/inhibitor/environment system, the mild steel surface is well understood by implying suitable isotherm that illustrates forecast information relevant to adsorption. [51, 52]. The inhibition efficiency is correlated with degree of surface coverage (θ) that was extracted from EIS results and the best fit was found to obey modified Langmuir adsorption isotherm. This behavior was observed to all compounds and the data were used at 30°C of temperature and 3 h of immersion time. The mechanism of adsorption over a metal surface was investigated for the synthesized inhibitors, and it was calculated, initially, from the Langmuir model equation, described in Equation (8), and illustrated by the plot in Figure 8.

$$\frac{C}{\theta} = \frac{1}{K_{ads}} + C, \tag{8}$$

where K_{ads} = equilibrium adsorption constant, C = inhibitor concentration and θ = degree of coverage. The degree of coverage (θ) is directly proportional to the corrosion inhibition efficiency, and it can be calculated according to Equation (9).

$$\theta = \frac{R_{ct} - R^0_{ct}}{R_{ct}}, \tag{9}$$

where R_{ct} = charge transfer resistances for the inhibitor agent and R^0_{ct}= charge transfer resistances for the blank solution. Table 8 shows the results of the correlation coefficients and slopes.

Table 8 shows that the slope values are outside of the ideal range for the Langmuir isotherm; therefore, a modification in the Langmuir model was performed according to the literature [53, 54] and can be seen in Equation (10).

$$\frac{C}{\theta} = \frac{n}{K_{ads}} + nC, \tag{10}$$

where n = correction parameter of slope and the other parameters remain the same.

The isotherm results enable the calculation of K_{ads} and ΔG_{ads} values of the system through Equation (11) and (10). The values of their K_{ads}, ΔG_{ads}, and slopes and the value of n are shown in Table 8, values obtained through the different concentrations studied and their degrees of coverage by the EIS technique.

$$\Delta G_{ads} = -RT \ln (55.55) K_{ads}, \tag{11}$$

where ΔG_{ads} = standard free energy of adsorption, K_{ads} = adsorption equilibrium constant, 55.55 = molar concentration of the water, R = universal gas constant, and T = temperature in K.

The information about the mechanism between inhibitor agents and metallic surface can be obtained by adsorption isotherm [55]. The surface coverage degree values obtained from the EIS measurements for the inhibitors fitted

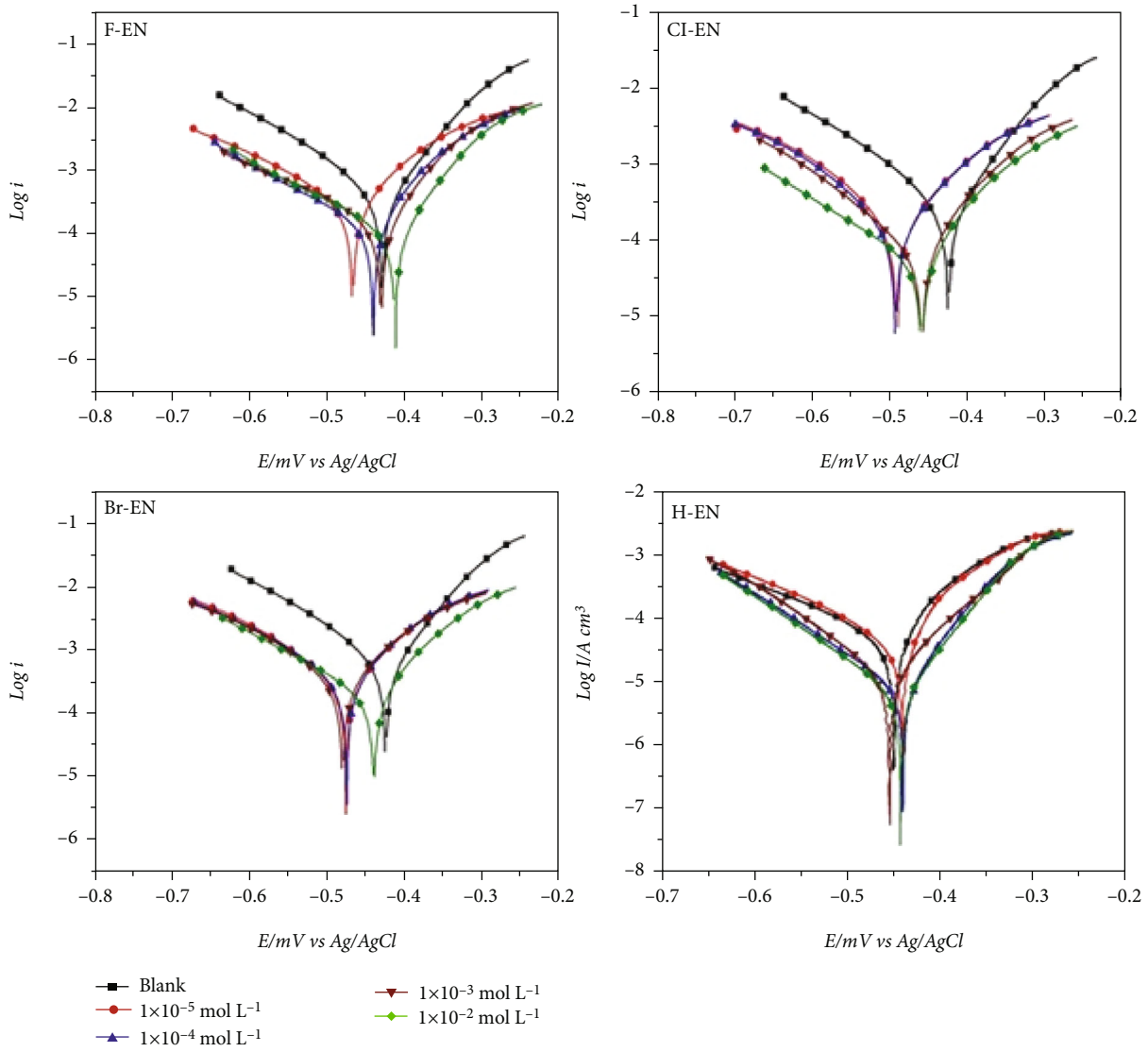

Figure 5: Polarization curves in absence and presence of inhibitors against AISI 1020 carbon steel in 1.0 mol L^{-1} HCl.

in Langmuir modification equation model, a straight line was obtained for the plot C/θ versus C, and nevertheless, the slopes observed for the compounds were differed from the ideal value of Langmuir isotherm, which is approximately 1, suggesting that each molecule of the synthesized inhibitors occupied more than one site of the metal surface. This interpretation was made from the hypothesis that there is more of one site for each β-enaminoester molecule due to its size and conformational structure when compared to other inhibitors, for example, triazole and Schiff base derivatives (n near 1) [8, 11]. This hypothesis can be applied to equilibrium of between enaminoester in solution and enaminoester adsorbed on surface. Therefore, a modification of the model was necessary, and according to the literature, this modification included a correction factor (n) for slope values that were out of usual Langmuir slope range [24, 25].

The high values of K_{ads} suggest that the mechanism is of adsorption in the medium between metal and inhibitor, leading to a more effective inhibition effect. In this way, the strong interaction between the inhibitors and the mild steel can be attributed to the presence of nitrogen and oxygen, also π-electrons in the enaminoesters [56–58]. Generally, ΔG_{ads} negative values are related to the existence of electrostatic type interactions between inhibitor and the charged metallic surface, and they indicate that the adsorption of the enaminoester on the metal is a spontaneous process and explains the stability of the adsorbed film formed by the inhibitors [59–61].

Therefore, as shown in Table 8, the more efficient compound F-EN showed the highest value of K_{ads} (2.00×10^4 L mol^{-1}) and most negative value of ΔG_{ads} (- 35.06 kJ mol^{-1}).

The presence of halogen atoms as substituents in benzene ring of enaminoesters increased the efficiencies of corrosion inhibition, when compared to unsubstituted, due the existence of their nonligand electron pairs that also can interact on metal surface by donating charge. Furthermore,

Table 4: Electrochemical parameters obtained by PP tests for enaminoesters in 1.0 mol L^{-1} HCl medium in AISI 1020 carbon steel.

Inhibitor	C_{inh} (Mol L^{-1})	E_{corr} vs. ag/AgCl (mV)	j_{corr} (mA cm^{-2})	β_a (mV dec^{-1})	$-\beta_c$ (mV dec^{-1})	θ	η_{PP} (%)
Blank	—	-479	0.314	71.43	101.45	—	—
F-EN	1.0×10^{-5}	-465.27	0.342	109.05	185.03	0.4013	40.2
	1.0×10^{-4}	-440.73	0.151	75.93	199.15	0.6175	63.9
	1.0×10^{-3}	-429.32	0.154	74.87	183.24	0.7393	74.5
	1.0×10^{-2}	-411.55	0.077	50.84	128.72	0.8548	84.8
Cl-EN	1.0×10^{-5}	-466.51	0,262	107.32	124.19	0.4497	45.3
	1.0×10^{-4}	-461.27	0.124	100.32	139.42	0.5017	50.4
	1.0×10^{-3}	-468.78	0.092	79.24	135.97	0,7709	76.8
	1.0×10^{-2}	-465.21	0.080	77.12	100.78	0.8436	83.8
Br-EN	1.0×10^{-5}	-462.28	0.153	100.84	157.2	0.5113	51.0
	1.0×10^{-4}	-461.52	0.132	102.04	156.86	0.5781	58.9
	1.0×10^{-3}	-467.85	0.112	104.04	144.05	0.6427	63.7
	1.0×10^{-2}	-444.45	0.0791	84.48	105.03	0.7481	75.3
H-EN	1.0×10^{-5}	-434.51	0.199	101.26	139.77	0.3939	39.4
	1.0×10^{-4}	-442.34	0.151	97.22	120.96	0.5167	51.7
	1.0×10^{-3}	-463.33	0.091	73.76	115.20	0.7104	71.0
	1.0×10^{-2}	-450.31	0.070	59.28	107.56	0.7764	78.9

Table 5: Results of weight loss assays of carbon steel AIS 1020 including corrosion rates (W_{corr}/mg cm^{-2} h^{-1}) in the absence and presence of inhibitors, and corrosion inhibition efficiencies (EI%) at 30°C with variation in immersion time.

Time (h)	Blank W_{corr} (mg cm^{-2} h^{-1})	Inhibitor							
		F-EN		Cl–EN		Br-EN		H-EN	
		W_{corr}	EI%	W_{corr}	EI%	W_{corr}	EI%	W_{corr}	EI%
3	1.359 ± 0.003	0.195 ± 0.014	85.6	0.219 ± 0.001	83.8	0.253 ± 0.001	81.4	0.271 ± 0.001	80.0
6	1.225 ± 0.006	0.140 ± 0.001	88.5	0.177 ± 0.001	85.5	0.176 ± 0.002	86.6	0.202 ± 0.001	85.5
24	1.116 ± 0.019	0.061 ± 0.001	94.6	0.055 ± 0.001	95.0	0.138 ± 0.004	87.7	0.105 ± 0.001	90.6
48	1.005 ± 0.014	0.015 ± 0.001	98.5	0.022 ± 0.001	97.8	0.021 ± 0.002	97.9	0.077 ± 0.001	92.4

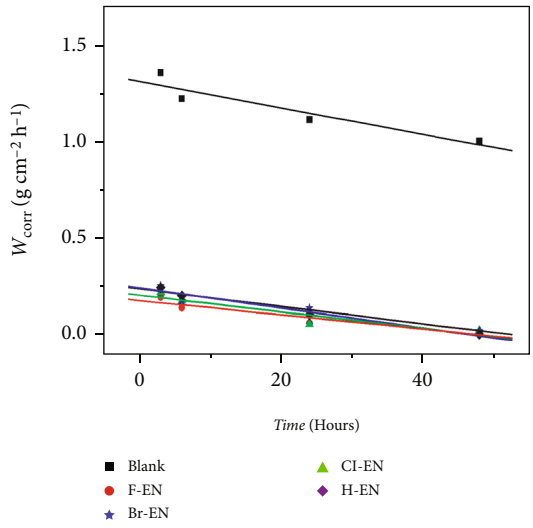

Figure 6: Graphic of W_{corr} versus immersion time for the halogenated enaminoesters synthesized against AISI 1020 carbon steel in 1.0 mol L^{-1} HCl solution in the absence and in the presence of inhibitors.

the resonance effect of these nonligand electron pairs with the double chemical bond and carbonyl moiety caused a higher delocalization of electron density that is favorable with the metal surface interaction. The increase of corrosion inhibition in different metals and alloys by the presence of halogen atoms in several compounds is very known and related in the literature as, for example, in the case of imidazole derivatives [62] and acridine derivatives [63], due to the role of electronic properties of halogens as indicated above.

3.7. Computational Methods. For the study of structural properties that influence the corrosion inhibition efficiency, theoretical calculations were performed using the SPARTAN-14 program. Using the semi-empirical method, the energies of the boundary molecular orbitals HOMO (higher energy occupied molecular orbital) and LUMO (lowest energy unoccupied molecular orbital), the $\Delta E_{LUMO-HOMO}$ and the dipole moment (μ) of the halogenated aniline β-enaminoesters (F-EN, Cl-EN, Br-EN, and H-EN) were calculated by the semi-empirical PM6 method. Table 9 shows the theoretical results obtained for the synthesized compounds and Figure 9 their optimized structures.

Table 6: Weight loss data for carbon steel AISI 1020 in 1.0 mol L^{-1} HCl solution in the absence and presence of inhibitors at 3 h of immersion time with variable temperature.

Temp (°C)	Blank W_{corr} (mg cm^{-2} h^{-1})	Inhibitor							
		F-EN		Cl-EN		Br–EN		H-EN	
		W_{corr}	EI%	W_{corr}	EI%	W_{corr}	EI%	W_{corr}	EI%
30	1.359	0.195	85.6	0.219	83.8	0.253	81.4	0.272	80.0
40	2.281	0.377	83.5	0.441	80.7	0.452	80.2	0.202	80.1
50	3.485	0.731	79.0	1.118	69.7	1.207	65.4	1.290	63.0
60	4.943	2.051	58.5	1.784	63.9	2.361	52.1	2.107	57.4

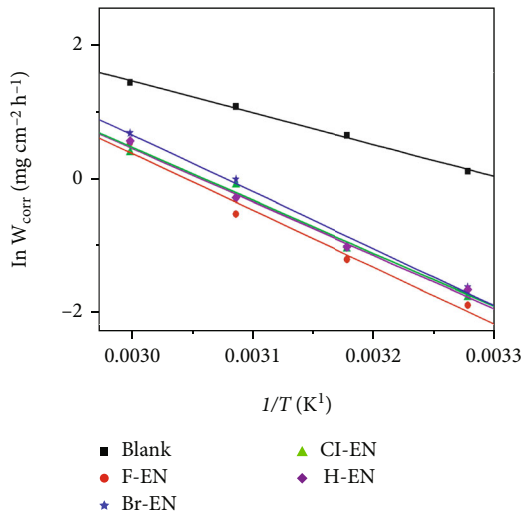

Figure 7: Arrhenius graph for AISI 1020 carbon steel in 1.0 mol L^{-1} HCl solution in the absence and presence of inhibitors.

Table 7: Values of E_a, $\triangle H^{\neq}_{ads}$, and $\triangle S^{\neq}_{ads}$ in the corrosion process of AISI 1020 carbon steel in 1.0 mol L^{-1} HCl, in the absence and presence of inhibitors.

Inhibitor	Correlation coefficient (r)	Slope	E_a (kJ Mol^{-1})	$\triangle H^{\neq}_{ads}$ (kJ Mol^{-1})	$\triangle S^{\neq}_{ads}$ (J Mol^{-1} K^{-1})
Blank	0.99684	14.47	35.56	33.47	-131.67
F-EN	0.99136	23.58	63.68	61.82	-55.26
Cl-EN	0.99458	22.55	59.77	57.95	-66.27
Br-EN	0.99614	23.85	63.69	61.81	-53.02
H-EN	0.99720	22.08	59.30	61.40	-50.28

The orbital theory provides important information about the corrosion inhibition efficiency of a compound, where the energy of HOMO is related to the molecule's ability to supply electrons. So, molecules with high E_{HOMO} values tend to donate electrons more easily to the metal's d orbitals. On the other hand, the energy of LUMO is associated with the molecule's ability to receive electrons, so as E_{LUMO} decreases, the inhibitor can receive electrons from the metal more easily [48]. Thus, can be observed that the lower value of E_{LUMO} showed by F-EN correlates with the best inhibitory efficiency indicating the importance of donating iron electrons to inhibitor agent. All molecules presented correlation between the inhibitory efficiency with the energy value of the LUMO orbital, that is, the lower the energy of the LUMO, the greater the efficiency. However, the values of the difference between frontier orbitals

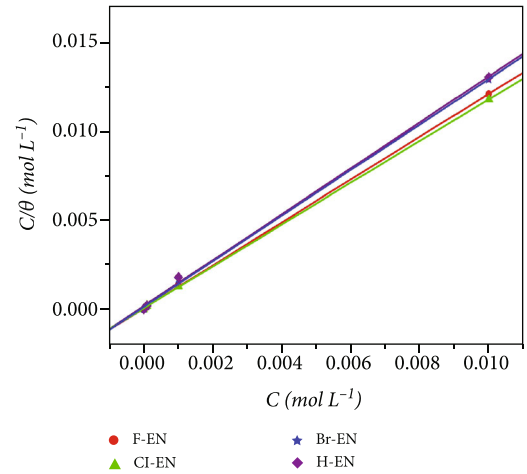

Figure 8: Langmuir adsorption isotherm plot for the inhibitors on carbon steel surface in 1.0 mol L^{-1} HCl.

Table 8: Values of parameters obtained from linearized Langmuir adsorption isotherm for the inhibitors on AISI 1020 carbon steel in 1.0 mol L^{-1} HCl using the electronic impedance spectroscopic data.

Inhibitor	Correlation coefficient (r)	Slope	n	K_{ads} (L Mol^{-1})	ΔG°_{ads} (kJ Mol^{-1})
F-EN	0.99999	1.17	0.85	2.00×10^4	-35.06
Cl-EN	0.99996	1.19	0.84	1.16×10^4	-33.69
Br-EN	0.99974	1.25	0.80	6.83×10^3	-32.36
H-EN	0.99995	1.26	0.80	1.06×10^4	-33.46

Table 9: Electronic properties of F-EN, Cl-EN, Br-EN, and H-EN obtained by semi-empirical PM6 method.

Inhibitor	E (eV)		$\Delta E_{LUMO-HOMO}$ (eV)	μ (D)
	HOMO	LUMO		
F-EN	- 8.84	- 0.36	8.48	5.44
Cl-EN	- 8.97	- 0.60	8.37	3.79
Br-EN	- 8.80	- 0.49	8.31	3.42
H-EN	- 8.95	- 0.70	8.25	1.58

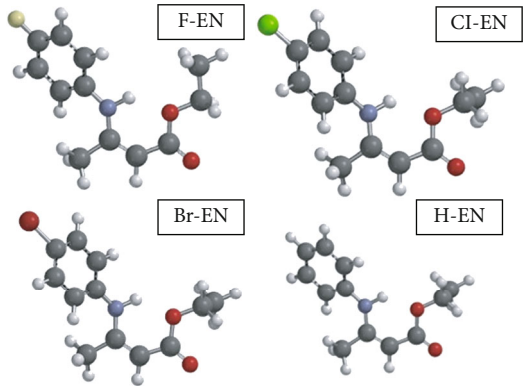

Figure 9: Optimized molecular structure of F-EN, Cl-EN, Br-EN, and H-EN.

($\Delta E_{\text{LUMO-HOMO}}$) did not correlate with the inhibition efficiency.

Another theoretical parameter used to evaluate the inhibition efficiency is the dipole moment (μ), that a measure of the asymmetry of the charge distribution in the molecule. Higher dipole moment values are associated to greater adsorption of the inhibitor agents and, consequently, increased the inhibition efficiency. Several works that support important anticorrosive effects also indicate high values of dipole moments indicating the delocalization of frontier orbitals [64, 65]. Thus, considering the experimental results, can be observed that they agree with the theoretical values of the dipole moment values, where F-EN > Cl-EN > Br-EN > H-EN correspond to inhibition efficiency order. The higher value of dipolar moment was obtained to F-EN (5.44 Debye) indicating greater delocalization of charge leading to substituting the water molecules on metal surface [66–68].

4. Conclusions

The corrosion process mostly affects metals, which tend to return to their most stable and least energetic form; hence, corrosion is directly linked to the high costs of replacing parts and maintaining equipment. Therefore, fostering the search for new corrosion inhibiting agents is critical.

In this work, it can be concluded that the synthesis of the enaminoesters occurred satisfactorily, presenting favorable yields, in the range of 68-81%, with facile workup and with easily accessible start material through ecofriendly technique.

The results of mass loss allowed us to conclude that the analyzed compounds have high anticorrosion activity against AISI 1020 carbon steel in 1.0 mol L^{-1} hydrochloric acid. F-EN was the most efficient among them, with 98% efficiency, at 30°C in 24 h immersion besides having the best inhibition efficiencies at 40°C and 50°C. These results were corroborated by the electrochemical techniques of EIS, LPR, and PP. Although the corrosion inhibition efficiency was not exceptional, the facility of compound preparation justifies the interest in this chemical class.

The thermodynamic parameters of E_a and $\triangle H^{\neq}_{ads}$ confirmed the compounds inhibitory activity, as there was an increase in these values compared to blank, indicating an increase in the energy barrier for the beginning of corrosion. Also, the $\triangle S^{\neq}_{ads}$ values confirmed inhibitory action, as they were less negative than blank, indicating deepening disorder in the system, which was already expected. Langmuir isotherm of adsorption was obeyed suggesting that the inhibitors form a monolayer film in metal surface.

With all the results taken into consideration, halogenated enaminoesters derived from aniline might be promising options for preventing corrosion of AISI 1020 carbon steel in acidic environment, and F-EN is the most efficient in the series.

Data Availability

The data (Excel and Origin 8.0) used to support the findings of this study are available from the authors by request.

Conflicts of Interest

The authors declare that have no conflicts of interest regarding the publication of this paper.

Acknowledgments

The authors are very grateful to Coordenação de Aperfeiçoamento de Pessoal de Nível Superior (CAPES), Conselho Nacional de Desenvolvimento Científico e Tecnológico (CNPq), and Petróleo Brasileiro (Petrobras) for financial support. This study was financed in part by the Coordenação de Aperfeiçoamento de Pessoal de Nível Superior - Brasil (CAPES) - Finance Code 001.

References

[1] D. Yang, Y. Yuwei, S. Yue, L. Shuang, G. Dirong, and Z. Haichao, "Functionalization of citric acid-based carbon dots by imidazole toward novel green corrosion inhibitor for carbon steel," *Journal of Cleaner Production*, vol. 229, pp. 180–192, 2019.

[2] A. H. Alamri and I. B. Obot, "Highly efficient corrosion inhibitor for C1020 carbon steel during acid cleaning in multistage flash (MSF) desalination plant," *Desalination*, vol. 470, pp. 114100–114115, 2019.

[3] V. N. Ayukayeva, G. I. Boiko, N. P. Lyubchenko et al., "Polyoxyethylene sorbitan trioleate surfactant as an effective corrosion inhibitor for carbon steel protection," *Colloids and Surfaces A: Physicochemical and Engineering Aspects*, vol. 579, article 123636, 2019.

[4] A. Valbon, M. A. Neves, and A. Echevarria, "Anticorrosive effect of PVP 40000 against AISI 1020 carbon steel in HCl," *Materials Research*, vol. 21, no. 6, article e20170847, 2018.

[5] M. Tavakkoli, C. Sung, J. Kuang, A. Chen, J. Hu, and F. M. Vargas, "Effect of carbon steel corrosion on asphaltene deposition," *Energy & Fuels*, vol. 33, no. 5, pp. 3808–3815, 2018.

[6] M. F. L. P. Carlos, A. Valbon, M. A. Neves, M. R. L. Santos, and A. Echevarria, "β-Enaminoesters as novel corrosion inhibitors for carbon steel in acidic medium," *Journal of the Brazilian Chemical Society*, vol. 29, no. 12, pp. 2542–2553, 2018.

[7] M. Sarvghad, D. Del Aguila, and G. Will, "Optimized corrosion performance of a carbon steel in dilute sulfuric acid

through heat treatment," *Applied Surface Science*, vol. 491, pp. 460–468, 2019.

[8] C. M. Fernandes, L. X. Alvarez, N. E. Santos, A. C. M. Barrios, and E. A. Ponzio, "Green synthesis of 1-benzyl-4-phenyl-1 *H*-1,2,3-triazole, its application as corrosion inhibitor for mild steel in acidic medium and new approach of classical electrochemical analyses," *Corrosion Science*, vol. 149, pp. 185–194, 2019.

[9] J. Chen, C. Wang, J. Han et al., "Corrosion inhibition performance of threonine-modified polyaspartic acid for carbon steel in simulated cooling water," *Journal of Applied Polymer Science*, vol. 136, no. 15, pp. 47242–47254, 2019.

[10] S. K. Ahmed, W. B. Ali, and A. A. Khadom, "Synthesis and characterization of new triazole derivatives as corrosion inhibitors of carbon steel in acidic medium," *Jounal of Bio and Tribo Corrosion*, vol. 5, no. 1, pp. 15–32, 2019.

[11] H. Heydari, M. Talebian, Z. Salarvand, K. Raeissi, M. Bagheri, and M. A. Golozar, "Comparison of two Schiff bases containing *O*-methyl and nitro substitutes for corrosion inhibiting of mild steel in 1 M HCl solution," *Journal of Molecular Liquids*, vol. 254, pp. 177–187, 2018.

[12] C. Frauches-Santos, M. A. Albuquerque, M. C. C. Oliveira, and A. Echevarria, "The corrosion and the anticorrosion agents," *Revista Virtual de Química*, vol. 6, no. 2, pp. 293–309, 2014.

[13] L. Zhou, Y. Lv, Y. Hu, J. Zhao, X. Xia, and X. Li, "Experimental and theoretical investigations of 1,3,5-tris(4-aminophenoxy)-benzene as an effective corrosion inhibitor for mild steel in 1 M HCl," *Journal of Molecular Liquids*, vol. 249, pp. 179–187, 2018.

[14] D. S. Chauhan, K. R. Ansari, A. A. Sorour, M. A. Quraishi, H. Lgaz, and R. Salghi, "Thiosemicarbazide and thiocarbohydrazide functionalized chitosan as ecofriendly corrosion inhibitors for carbon steel in hydrochloric acid solution," *International Journal of Biological Macromolecules*, vol. 107, Part B, pp. 1747–1757, 2018.

[15] H. Ju, X. Li, N. Cao, F. Wang, Y. Liu, and Y. Li, "Schiff-base derivatives as corrosion inhibitors for carbon steel materials in acid media: quantum chemical calculations," *Corrosion Engineering Science and Technology*, vol. 53, no. 1, pp. 36–43, 2018.

[16] S. Yaragorla and A. Pareek, "Regioselective intramolecular annulations of ambident β-enamino esters: a diversity-oriented synthesis of nitrogen-containing privileged molecules," *Tetrahedron Letters*, vol. 59, no. 10, pp. 909–913, 2018.

[17] G. Negri, C. Kascheres, and A. J. Kascheres, "Recent development in preparation reactivity and biological activity of enaminoketones and enaminothiones and their utilization to prepare heterocyclic compounds," *Journal of Heterocyclic Chemistry*, vol. 41, no. 4, pp. 461–491, 2004.

[18] B. Stanovnik, "Enaminone, enaminoesters, and related compounds in the metal-free synthesis of pyridines and fused pyridines," *European Journal of Organic Chemistry*, vol. 2019, no. 31-32, pp. 5120–5132, 2019.

[19] M. Xingxing, X. Yu, H. Huang, Y. Zho, and Q. Song, "Synthesis of thiazoles and isothiazoles via three-component reaction of enaminoesters, sulfur, and bromodifluoroacetamides/esters," *Organic Letters*, vol. 22, no. 14, pp. 5284–5288, 2020.

[20] D. Magoo, K. Aggarwal, S. Gupta, and K. Meena, "Enamines and their variants as intermediates for synthesis of aza-heterocycles with applications in MCRs," *Tetrahedron*, vol. 103, article 132545, 2022.

[21] A. Gharib, M. Jahangir, and M. Roshani, "Catalytic synthesis of ethyl β-arylamino crotonates and 2-methyl-4-quinolone using preyssler heteropolyacid, H14[NaP5W30O110] and it's supported as catalysts," in *Proceedings of The 12th International Electronic Conference on Synthetic Organic Chemistry*, 2008.

[22] N. Wlodarczyk, C. Simenel, M. Delepierre, J. C. Barale, and Y. L. Janin, "On the Knorr synthesis of 6-bromo-4-methylquinolin-2(1H)-one," *Synthesis*, vol. 2011, no. 6, pp. 934–942, 2011.

[23] B. Medapi, J. Renuka, S. Saxena et al., "Design and synthesis of novel quinoline-aminopiperidine hybrid analogues as *Mycobacterium tuberculosis* DNA gyraseB inhibitors," *Bioorganic & Medicinal Chemistry*, vol. 23, no. 9, pp. 2062–2078, 2015.

[24] A. Singh, K. R. Ansari, M. A. Quraishi, and S. Kaya, "Theoretically and experimentally exploring the corrosion inhibition of N80 steel by pyrazol derivatives in simulated acidizing environment," *Journal of Molecular Structure*, vol. 1206, pp. 127685–127723, 2020.

[25] E. Ituen, A. James, O. Akaranta, and S. Sun, "Eco-friendly corrosion inhibitor from *Pennisetum purpureum* biomass and synergistic intensifiers for mild steel," *Chinese Journal of Chemical Engineering*, vol. 24, no. 10, pp. 1442–1447, 2016.

[26] I. B. Obot, D. D. Macdonald, and Z. M. Gasem, "Density functional theory (DFT) as a powerful tool for designing new organic corrosion inhibitors. Part 1: An overview," *Corrosion Science*, vol. 99, pp. 1–30, 2015.

[27] A. Valbon, M. A. Neves, and A. Echevarria, "Experimental and theoretical evaluation of asymmetric thioureas on the corrosion of carbon steel in acidic medium," *International Journal of Electrochemical Science*, vol. 12, pp. 3072–3087, 2017.

[28] A. K. Singh, B. Chugh, M. Singh et al., "Hydroxy phenyl hydrazides and their role as corrosion impeding agent: a detail experimental and theoretical study," *Journal of Molecular Liquids*, vol. 330, pp. 115605–115623, 2021.

[29] N. Labjar, M. Lebrini, F. Bentiss, N. E. Chihib, S. E. Hajjaji, and C. Jama, "Corrosion inhibition of carbon steel and antibacterial properties of aminotris-(methylenephosphonic) acid," *Materials Chemistry and Physics*, vol. 119, no. 1-2, pp. 330–336, 2010.

[30] J. Gopal, P. Dwivedi, S. Sundaram, and R. Prakash, "Inhibitive effect of *Chlorophytum borivilianum* root extract on mild steel corrosion in HCl and H_2SO_4 solutions," *Industrial & Engineering Chemistry Research*, vol. 52, no. 31, pp. 10673–10681, 2013.

[31] L. Li, Q. Qu, W. Bai et al., "Sodium diethyldithiocarbamate as a corrosion inhibitor of cold rolled steel in 0.5 M hydrochloric acid solution," *Corrosion Science*, vol. 59, pp. 249–257, 2012.

[32] Q. Q. Liao, Z. W. Yue, D. Yang et al., "Self-assembled monolayer of ammonium pyrrolidine dithiocarbamate on copper detected using electrochemical methods, surface enhanced Raman scattering and quantum chemistry calculations," *Thin Solid Films*, vol. 519, no. 19, pp. 6492–6498, 2011.

[33] H. Lgaz, K. Subrahmanya Bhat, R. Salghi et al., "Insights into corrosion inhibition behavior of three chalcone derivatives for mild steel in hydrochloric acid solution," *Journal of Molecular Liquids*, vol. 238, pp. 71–83, 2017.

[34] A. Valbon, B. F. Ribeiro, M. A. F. Soares, M. C. C. Oliveira, M. A. Neves, and A. Echevarria, "Extrato de hibisco-colibri como inibidor verde de corrosão do aço-carbono em ácido sulfúrico," *Química Nova*, vol. 42, no. 7, pp. 797–802, 2019.

[35] N. I. Kairi and J. Kassim, "The effect of temperature on the corrosion inhibition of mild steel in 1 M HCl solution by *Curcuma longa* extract," *International Journal of Electrochemical Science*, vol. 8, no. 5, pp. 7138–7155, 2013.

[36] V. V. Torres, V. A. Rayol, M. Magalhães et al., "Study of thioureas derivatives synthesized from a green route as corrosion inhibitors for mild steel in HCl solution," *Corrosion Science*, vol. 79, pp. 108–118, 2014.

[37] B. Chugh, A. K. Singh, S. Thakur et al., "An exploration about the interaction of mild steel with hydrochloric acid in the presence of N-(benzo[d]thiazole-2-yl)-1-phenylethan-1-imines," *The Journal of Physical Chemistry C*, vol. 123, no. 37, pp. 22897–22917, 2019.

[38] B. Fan, Y. Ma, M. Wang et al., "Revealing the assembly mechanism of an octadecylamine based supramolecular complex on mild steel in condensate water: correlative experimental and theoretical studies," *Journal of Molecular Liquids*, vol. 292, article 111446, 2019.

[39] H. Liu, B. Fan, Z. Liu, B. Yang, X. Zheng, and H. Hao, "Electronic effects on protective mechanism of electropolymerized coatings based on *N*-substituted aniline derivatives for mild steel in saline solution," *Journal of Industrial and Engineering Chemistry*, vol. 106, pp. 297–310, 2022.

[40] B. Fan, H. Hao, B. Yang, and Y. Li, "Insights into the inhibition mechanism of a novel supramolecular complex towards the corrosion of mild steel in the condensate water: experimental and theoretical studies," *Research Chemical Intermediates*, vol. 44, no. 10, pp. 5711–5736, 2018.

[41] S. Sheetal, M. S. Sengupta, M. Singh et al., "An insight about the interaction of Aryl Benzothiazoles with mild steel surface in aqueous HCl solution," *Journal of Molecular Liquids*, vol. 354, pp. 118890–118903, 2022.

[42] B. Chugh, A. K. Singh, D. Poddar, S. Thakur, B. Pani, and P. Jain, "Relation of degree of substitution and metal protecting ability of cinnamaldehyde modified chitosan," *Carbohydrate Polymers*, vol. 234, pp. 115945–115955, 2020.

[43] M. Faustin, A. Maciuk, P. Sauvin, C. Roos, and M. Lebrini, "Corrosion inhibition of C38 steel by alkaloids extract of *Geissospermum laeve* in 1 M hydrochloric acid: Electrochemical and phytochemical studies," *Corrosion Science*, vol. 92, pp. 287–300, 2015.

[44] S. M. Taufik and N. A. Negm, "Synthesis, characterization and evaluation of some anionic surfactants with phosphate group as a biodegradable corrosion inhibitor for carbon steel in acidic solution," *Journal of Molecular Liquids*, vol. 215, pp. 185–196, 2016.

[45] I. B. Barros, M. A. A. Kappel, P. M. Santos, V. F. Veiga Junior, E. D'Elia, and I. N. Bastos, "The inhibitory action of Bauhinia purpurea extracts on the corrosion of carbon steel in sulfuric acid medium," *Materials Research*, vol. 19, no. 1, pp. 187–194, 2016.

[46] R. S. Nathiya and V. Ray, "Evaluation of *Dryopteris cochleata* leaf extracts as green inhibitor for corrosion of aluminium in 1 M H2SO4," *Egyptian Journal Petroleum*, vol. 26, no. 2, pp. 313–323, 2017.

[47] L. C. Murulana, M. M. Kabanda, and E. E. Ebenso, "Investigation of the adsorption characteristics of some selected sulphonamide derivatives as corrosion inhibitors at mild steel/hydrochloric acid interface: Experimental, quantum chemical and QSAR studies," *Journal of Molecular Liquids*, vol. 215, pp. 763–779, 2016.

[48] M. Prajila and A. Joseph, "Controlling the rate of dissolution of mild steel in sulfuric acid through the adsorption and inhibition characteristics of (4-(4-Hydroxybenzylideneamino)-4H-1,2,4-Triazole-3,5-diyl)dimethanol (HATD)," *Journal of Bio- and Tribo-Corrosion*, vol. 3, no. 1, pp. 3–10, 2017.

[49] E. A. Badr, M. A. Bedair, and S. M. Shaban, "Adsorption and performance assessment of some imine derivatives as mild steel corrosion inhibitors in 1.0 M HCl solution by chemical, electrochemical and computational methods," *Materials Chemistry and Physics*, vol. 219, pp. 444–460, 2018.

[50] G. O. Resende, S. F. Teixeira, I. F. Figueiredo et al., "Synthesis of 1,2,3-triazole derivatives and its evaluation as inhibitors for carbon steel," *International Journal of Electrochemistry*, vol. 2019, Article ID 6759478, 12 pages, 2019.

[51] B. Chugh, S. Thakur, B. Pani et al., "Investigation of phenol-formaldehyde resins as corrosion impeding agent in acid solution," *Journal of Molecular Liquids*, vol. 330, pp. 115649–115667, 2021.

[52] A. S. Fouda, A. F. Hassan, M. A. Elmorsi, T. A. Fayed, and A. Abdelhakim, "Chalcones as environmentally-friendly corrosion inhibitors for stainless steel type 304 in 1 M HCl solutions," *International Journal of Electrochemical Science*, vol. 9, pp. 1298–1320, 2014.

[53] R. F. V. Villami, P. Corio, J. C. Rubim, and S. M. L. Agostinho, "Sodium dodecylsulfate-benzotriazole synergistic effect as an inhibitor of processes on copper | chloridric acid interfaces," *Journal of Electroanalytical Chemistry*, vol. 535, no. 1-2, pp. 75–83, 2002.

[54] R. Karthikaiselvi and S. Subhashini, "The water soluble composite poly(vinylpyrrolidone-methylaniline): a new class of corrosion inhibitors of mild steel in hydrochloric acid media," *Arabian Journal of Chemistry*, vol. 10, no. S1, pp. S627–S635, 2017.

[55] X. Li, S. Deng, and H. Fu, "Triazolyl blue tetrazolium bromide as a novel corrosion inhibitor for steel in HCl and H_2SO_4 solutions," *Corrosion Science*, vol. 53, no. 1, pp. 302–309, 2011.

[56] R. S. Erami, M. Amirnasr, S. Meghdadi, M. Talebian, H. Farrokhpour, and K. Raeissi, "Carboxamide derivatives as new corrosion inhibitors for mild steel protection in hydrochloric acid solution," *Corrosion Science*, vol. 151, pp. 190–197, 2019.

[57] A. M. Badiea and K. N. Mohana, "Effect of temperature and fluid velocity on corrosion mechanism of low carbon steel in presence of 2-hydrazino-4,7-dimethylbenzothiazole in industrial water medium," *Corrosion Science*, vol. 51, no. 9, pp. 2231–2241, 2009.

[58] F. Bentiss, M. Lebrini, and M. Lagrenée, "Thermodynamic characterization of metal dissolution and inhibitor adsorption processes in mild steel/2,5-bis(*n*-thienyl)-1,3,4-thiadiazoles/hydrochloric acid system," *Corrosion Science*, vol. 47, no. 12, pp. 2915–2931, 2005.

[59] B. Chugh, A. K. Singh, A. Chaouiki, R. Salghi, S. Thakur, and B. Pani, "A comprehensive study about anti-corrosion behaviour of pyrazine carbohydrazide: gravimetric, electrochemical, surface and theoretical study," *Journal of Molecular Liquids*, vol. 299, pp. 112160–112177, 2020.

[60] A. K. Singh and M. A. Quraishi, "Effect of Cefazolin on the corrosion of mild steel in HCl solution," *Corrosion Science*, vol. 52, no. 1, pp. 152–160, 2010.

[61] I. Ahamad, R. Prasad, and M. A. Quaraishi, "Adsorption and inhibitive properties of some new Mannich bases of isatin

derivatives on corrosion of mild steel in acidic media," *Corrosion Science*, vol. 52, no. 4, pp. 1472–1481, 2010.

[62] I. Abdulazeez, A. Zeino, C. W. Kee et al., "Mechanistic studies of the influence of halogen substituents on the corrosion inhibitive efficiency of selected imidazole molecules: a synergistic computational and experimental approach," *Applied Surface Science*, vol. 471, pp. 494–505, 2019.

[63] W. Zhang, H. -J. Li, M. Wang, L. -J. Wang, F. Shang, and Y. -C. Wu, "Halogen-substituted acridines as highly effective corrosion inhibitors for mild steel in acid medium," *The Journal of Physical Chemistry C*, vol. 122, no. 44, pp. 25349–25364, 2018.

[64] H. Liu, B. Fan, G. Fan, Y. Ma, H. Hao, and H. Zhang, "Anticorrosive mechanism of poly (*N*-ethylaniline)/sodium silicate electrochemical composites for copper: correlated experimental and *in-silico* studies," *Journal of Material Sciences & Technologies*, vol. 72, pp. 202–216, 2021.

[65] C. D. Taylor, "Corrosion informatics: an integrated approach to modelling corrosion," *Corrosion Engineering, Science and Technology*, vol. 50, no. 7, pp. 490–508, 2015.

[66] M. Hosseini-Sarvari, "Nano-tube TiO_2 as a new catalyst for eco-friendly synthesis of imines in sunlight," *Chinese Chemical Letters*, vol. 22, no. 5, pp. 547–550, 2011.

[67] H. Liu, B. Fan, G. Fan et al., "Long-term protective mechanism of poly(N-metylaniline)/phosphate one step electropolymerized coatings for copper in 3.5% NaCl solution," *Journal of Alloys and Compounds*, vol. 872, article 150752, 2021.

[68] M. P. Carlos, N. F. Xavier Jr., A. M. Silva Jr., M. A. Neves, A. Echevarria, and G. F. Bauerfeldt, "Synergy between experimental and theoretical investigations reveals the anticorrosion efficiency of imine-chalcones," *Journal of Brazilian Chemical Society*, vol. 32, no. 8, pp. 1654–1669, 2021.